# Development of a Three-Dimensional HYDRO Code (HYDRO-RPI/3D) for the Hydrodynamic Simulation of Single Bubble Sonoluminescence (SBSL)

Kenneth Jansen
Richard T. Lahey, Jr.
Center for Multiphase Research
Rensselaer Polytechnic Institute
Troy, NY USA



#### INTRODUCTION

The three-dimensional (3D) numerical simulation of both Single Bubble Sonoluminescence (SBSL) and Multi-Bubble Sonoluminescence (MBSL) phenomena allows one to study the bubble instability mechanisms which may limit the achievement of ultra-high gas temperatures for bubble fusion and other important applications (e.g., sonochemistry).

The HYDRO-RPI/3D code allows for the direct numerical simulation (DNS) of three-dimensional bubble dynamics. The calculation domain consists of two regions separated by a vapor/liquid interface. The two regions have different densities, velocities, and temperatures, which are determined by separate conservation and state equations.

One of the major challenges in the development of HYDRO-RPI/3D was how to handle shocks and the moving interface. Depending on the circumstances at the interface, one can use either a moving mesh method or a fixed mesh method (with interface-capturing capability). A moving mesh method typically requires discretization of the liquid and gas domain separately and computation of the motion of the interface by moving the mesh for each time step to reflect the current configuration (e.g., arbitrary Lagrangian-Eulerian methods: Hirt et al. [1], Donea [2], Hughes et al. [3], and Liu & Belytschoko [4]; stabilized space-time finite element methods: Tezduyar et al. [5-6], in which remeshing is needed when the mesh distortion becomes too high).

In 3D simulations, especially those based on parallel computing, reducing the frequency of automatic remeshing becomes essential, because the cost of too frequent 3D

automatic mesh generation becomes prohibitive. When the interface is complex and very unsteady reducing the frequency of mesh generation becomes a difficult task, and sometimes it is not possible. In such cases, interface-capturing methods with fixed meshes have been used. These interface-capturing methods are more flexible but yield less accurate representation of the interface compared to moving mesh methods.

The spatial discretization methods used in HYDRO-RPI/3D are based on finite element methods which are available for application with unstructured grids. In particular, the Galerkin/Least-Squares method of Hughes et al. [7-8], or the Streamline Upwind Petrov-Galerkin method (SUPG) method of Franca and Hughes [9]. They have proven to be stable and higher order accurate for flows ranging from inviscid to viscous. In HYDRO-RPI/3D, we solve, over the non-moving mesh, the conservation equations in each phase together with a transport equation governing the evolution of the phase indicator function, which identifies the two fluids. One of the objectives in this work is to accurately resolve and advect the interface between the two phases. To increase the accuracy in representing the interface, we use an adaptive grid corresponding to enhanced discretization at, or near, the moving interface.

## THE GOVERNING EQUATIONS

This section summarizes the conservation equations which are numerically evaluated in HYDRO-RPI/3D. These computations involve the solution of the transient Navier-Stokes equations of compressible flow. The conservation equations for phase-k may be written in Cartesian coordinates as:

Mass Conservation

$$\frac{\partial \mathbf{r}_k}{\partial t} + \frac{\partial \mathbf{r}_k u_k}{\partial x} + \frac{\partial \mathbf{r}_k v_k}{\partial y} + \frac{\partial \mathbf{r}_k w_k}{\partial z} = 0 \tag{1}$$

**Momentum Conservation** 

$$\frac{\partial \mathbf{r}_{k} u_{k}}{\partial t} + \left(\frac{\partial \mathbf{r}_{k} u_{k}^{2}}{\partial x} + \frac{\partial \mathbf{r}_{k} u_{k} v_{k}}{\partial y} + \frac{\partial \mathbf{r}_{k} u_{k} w_{k}}{\partial z}\right) + \frac{\partial p_{k}}{\partial x} = \left(\frac{\partial \mathbf{t}_{xx,k}}{\partial x} + \frac{\partial \mathbf{t}_{xy,k}}{\partial y} + \frac{\partial \mathbf{t}_{xz,k}}{\partial z}\right) + \mathbf{r}_{k} g_{x}$$
(2)

$$\frac{\partial \mathbf{r}_{k} \mathbf{v}_{k}}{\partial t} + \left( \frac{\partial \mathbf{r}_{k} u_{k} \mathbf{v}_{k}}{\partial x} + \frac{\partial \mathbf{r}_{k} \mathbf{v}_{k}^{2}}{\partial y} + \frac{\partial \mathbf{r}_{k} \mathbf{v}_{k} w_{k}}{\partial z} \right) + \frac{\partial p_{k}}{\partial y} = \left( \frac{\partial \mathbf{t}_{yx,k}}{\partial x} + \frac{\partial \mathbf{t}_{yy,k}}{\partial y} + \frac{\partial \mathbf{t}_{yz,k}}{\partial z} \right) + \mathbf{r}_{k} \mathbf{g}_{y}$$
(3)

$$\frac{\partial \mathbf{r}_{k} w_{k}}{\partial t} + \left( \frac{\partial \mathbf{r}_{k} w_{k} u_{k}}{\partial x} + \frac{\partial \mathbf{r}_{k} w_{k} v_{k}}{\partial y} + \frac{\partial \mathbf{r}_{k} w_{k}^{2}}{\partial z} \right) + \frac{\partial p_{k}}{\partial z} = \left( \frac{\partial \mathbf{t}_{zx,k}}{\partial x} + \frac{\partial \mathbf{t}_{zy,k}}{\partial y} + \frac{\partial \mathbf{t}_{zz,k}}{\partial z} \right) + \mathbf{r}_{k} g$$
(4)

Energy Conservation

$$\frac{\partial \mathbf{r}_{k} e_{k}}{\partial t} + \left(\frac{\partial \mathbf{r}_{k} u_{k} e_{k}}{\partial x} + \frac{\partial \mathbf{r}_{k} v_{k} e_{k}}{\partial x} + \frac{\partial \mathbf{r}_{k} w_{k} e_{k}}{\partial x}\right) + \left(\frac{\partial p_{k} u_{k}}{\partial x} + \frac{\partial p_{k} v_{k}}{\partial y} + \frac{\partial p_{k} w_{k}}{\partial z}\right) = 0$$

$$\frac{\partial}{\partial x} \left( \boldsymbol{t}_{xx,k} u_k + \boldsymbol{t}_{xy,k} v_k + \boldsymbol{t}_{xz,k} w_k \right) + \frac{\partial}{\partial y} \left( \boldsymbol{t}_{yx,k} u_k + \boldsymbol{t}_{yy,k} v_k + \boldsymbol{t}_{yz,k} w_k \right)$$

$$+\frac{\partial}{\partial z} \left( \boldsymbol{t}_{zx,k} u_k + \boldsymbol{t}_{zy,k} v_k + \boldsymbol{t}_{zz,k} w_k \right) - \left( \frac{\partial q_{x,k}''}{\partial x} + \frac{\partial q_{y,k}''}{\partial y} + \frac{\partial q_{z,k}''}{\partial z} \right)$$

$$+\mathbf{r}_{k}\left(u_{k}g_{x}+v_{k}g_{x}+w_{k}g_{x}\right)+q_{k}^{"''}\tag{5}$$

In these equations,  $r_k$  is the density;  $u_k$ ,  $v_k$  and  $w_k$  are the velocity components in the x, y and z directions, respectively;  $p_k$  is the static pressure;

 $t_{xx,k}$ ,  $t_{xy,k}$ ,  $t_{xz,k}$ ,  $t_{yy,k}$ ,  $t_{yz,k}$  and  $t_{zz,k}$  are the components of viscous stress;  $e_k$  is the specific total energy given by,

$$e_k = \frac{1}{2} \left( u_k^2 + v_k^2 + w_k^2 \right) + \mathbf{e}$$
 (6)

where  $\varepsilon$  is the specific internal energy;  $q''_{x,k}$ ,  $q''_{y,k}$  and  $q''_{z,k}$  are the x, y, and z components of the energy flux due to both heat conduction and mass diffusion;  $q'''_k$  is a volumetric heat source.

The constitutive equation for a Newtonian fluid relates the viscous stress tensor to the rate of strain tensor as:

$$t_{xx,k} = 2 \, \mathbf{m}_{k} \, \frac{\partial u_{k}}{\partial x} + \mathbf{I}_{k} \left( \frac{\partial u_{k}}{\partial x} + \frac{\partial v_{k}}{\partial y} + \frac{\partial w_{k}}{\partial z} \right),$$

$$t_{yy,k} = 2 \, \mathbf{m}_{k} \, \frac{\partial v_{k}}{\partial y} + \mathbf{I}_{k} \left( \frac{\partial u_{k}}{\partial x} + \frac{\partial v_{k}}{\partial y} + \frac{\partial w_{k}}{\partial z} \right),$$

$$t_{zz,k} = 2 \, \mathbf{m}_{k} \, \frac{\partial w_{k}}{\partial z} + \mathbf{I}_{k} \left( \frac{\partial u_{k}}{\partial x} + \frac{\partial v_{k}}{\partial y} + \frac{\partial w_{k}}{\partial z} \right),$$

$$t_{xy,k} = t_{yx,k} = \mathbf{m}_{k} \left( \frac{\partial u_{k}}{\partial x} + \frac{\partial v_{k}}{\partial y} \right),$$

$$t_{yz,k} = t_{zy,k} = \mathbf{m}_{k} \left( \frac{\partial v_{k}}{\partial x} + \frac{\partial w_{k}}{\partial y} \right), \text{ and,}$$

$$t_{zx,k} = t_{xz,k} = \mathbf{m}_{k} \left( \frac{\partial w_{k}}{\partial x} + \frac{\partial u_{k}}{\partial y} \right),$$

$$(7)$$

where  $m_k$  and  $l_k$  are the first and second coefficients of viscosity, respectively.

The energy flux components are given by:

$$q_{x,k}'' = -k_k \frac{\partial T_k}{\partial x} - \sum_i \mathbf{r}_k h_i D_i \frac{\partial (\mathbf{r}_i / \mathbf{r}_k)}{\partial x},$$

$$q_{y,k}'' = -k_k \frac{\partial T_k}{\partial y} - \sum_i \mathbf{r}_k h_i D_i \frac{\partial (\mathbf{r}_i / \mathbf{r}_k)}{\partial y}, \text{ and,}$$

$$q_{z,k}'' = -k_k \frac{\partial T_k}{\partial z} - \sum_i \mathbf{r}_k h_i D_i \frac{\partial (\mathbf{r}_i / \mathbf{r}_k)}{\partial z}.$$
(8)

where  $k_k$  is the thermal conductivity,  $T_k$  is the temperature,  $h_i$  is the specific enthalpy of species-i,  $D_i$  is the effective binary diffusion coefficient for species-i in the mixture, and mass conservation requires that the sum of the species densities should equal the density of the mixture, i.e.

$$\mathbf{r}_k = \sum_{i} \mathbf{r}_i \tag{9}$$

The first term in Eq. (8) is the energy flux due to thermal conductivity, while the second term is the energy flux due to diffusion of the species. For this later term, Fick's law has been used to describe the effect of diffusion. The equations of state which are valid for highly compressed fluids are of the form (Bae et al. [10]):

$$p_k = p_k(\mathbf{r}_k, T_k), \text{ and, } \mathbf{e}_k = \mathbf{e}_k(\mathbf{r}_k, T_k)$$
 (10)

The specific heats of the fluids mixture at constant pressure and constant volume are given by:

$$c_{p,k} = \frac{1}{\mathbf{r}_k} \sum_{i} c_{p_i} \mathbf{r}_i, \text{and}, c_{v,k} = \frac{1}{\mathbf{r}_k} \sum_{i} c_{v_i} \mathbf{r}_i.$$
 (11)

where  $c_{p_i}$  and  $c_{v_i}$  are the specific heats for species-i at constant pressure and constant volume, respectively.

The motion of the individual species in phase-k are determined through the mass diffusion equation:

$$\frac{\partial \mathbf{r}_i}{\partial t} + \frac{\partial \mathbf{r}_i u_k}{\partial x} + \frac{\partial \mathbf{r}_i v_k}{\partial y} + \frac{\partial \mathbf{r}_i w_k}{\partial z} =$$

$$\frac{\partial}{\partial x} \left[ \mathbf{r}_{k} D_{i} \frac{\partial}{\partial x} (\mathbf{r}_{i} / \mathbf{r}_{k}) \right] + \frac{\partial}{\partial y} \left[ \mathbf{r}_{k} D_{i} \frac{\partial}{\partial y} (\mathbf{r}_{i} / \mathbf{r}_{k}) \right] + \frac{\partial}{\partial z} \left[ \mathbf{r}_{k} D_{i} \frac{\partial}{\partial z} (\mathbf{r}_{i} / \mathbf{r}_{k}) \right]$$
(12)

If we sum Eq. (12) over all the species and use Eq. (9) with the mixture continuity equation, Eq. (1), we obtain the result that:

$$\sum_{i} \left\{ \frac{\partial}{\partial x} \left[ \mathbf{r}_{k} D_{i} \frac{\partial}{\partial x} (\mathbf{r}_{i} / \mathbf{r}_{k}) \right] + \frac{\partial}{\partial y} \left[ \mathbf{r}_{k} D_{i} \frac{\partial}{\partial y} (\mathbf{r}_{i} / \mathbf{r}_{k}) \right] + \frac{\partial}{\partial z} \left[ \mathbf{r}_{k} D_{i} \frac{\partial}{\partial z} (\mathbf{r}_{i} / \mathbf{r}_{k}) \right] \right\} = 0 \quad (13)$$

Equation (13) states that molecular diffusion alone produces not net mass transfer, hence no-change in the mixture density.

A phase indicator function,  $\Phi$ , serves as a marker identifying each fluid with the definition  $\Phi = \{1 \text{ for liquid, } k = 1, \text{ and } 0 \text{ for gas, } k=2\}$ . The interface between the two fluids is often approximated to be at  $\Phi = 0.5$ . The evolution of the interface function,  $\Phi$ , is governed by a time-dependent advection equation:

$$\frac{\partial \Phi}{\partial t} + u_I \frac{\partial \Phi}{\partial x} + v_I \frac{\partial \Phi}{\partial y} + w_I \frac{\partial \Phi}{\partial z} = 0 \tag{14}$$

where  $u_I$ ,  $v_I$  and  $w_I$  are the interface velocity components in the x, y and z directions, respectively. How accurately this law will be modeled will depend on how accurately the boundary between  $\Phi = 1$  and  $\Phi = 0$  is represented and advected.

The governing equations given above can be applied to each phase up to an interface, but not across it. A particular form of the balance equation should be used at an interface in order to take into account the "jump" (i.e., the sharp changes or discontinuities) in the various variables.

The interfacial mass balance equation is given by:

$$\sum_{k=1}^{2} \mathbf{r}_{k} \left( \underline{\mathbf{v}}_{k} - \underline{\mathbf{v}}_{i} \right) \Box \underline{\mathbf{n}}_{k} = 0, \text{ liquid phase for } \mathbf{k} = 1 \text{ and gas phase for } \mathbf{k} = 2. \quad (15)$$

We note  $\underline{n}_1 = -\underline{n}_2$ , where  $\underline{n}_1$  and  $\underline{n}_2$  are the outward unit normal vectors from the interface between phases 1 and 2. We have from Eq. (15),

$$\underline{\mathbf{v}}_{i} \Box \underline{n}_{1} = \frac{\left(\mathbf{r}_{1} \underline{\mathbf{v}}_{1} - \mathbf{r}_{2} \underline{\mathbf{v}}_{2}\right)}{\mathbf{r}_{1} - \mathbf{r}_{2}} \Box \underline{n}_{1}.$$
(16)

Noting that the interfacial mass flux from the  $k_{th}$  phase (due to phase change) is:

$$\Gamma_k \equiv \mathbf{r}_k \left( \underline{\mathbf{v}}_k - \underline{\mathbf{v}}_I \right) \Box \underline{n}_k \tag{17}$$

where,

$$\sum_{k=1}^{2} \Gamma_k = 0 \tag{18}$$

Substituting Eqs. (16) and (17), we have

$$\underline{\mathbf{v}}_{1} \square \underline{n}_{1} = \underline{\mathbf{v}}_{2} \square \underline{n}_{1} + \frac{(\mathbf{r}_{1} - \mathbf{r}_{2})}{\mathbf{r}_{1} \mathbf{r}_{2}} \Gamma_{1}$$
(19)

The interfacial energy balance is given by:

$$\Gamma_1 = \frac{\left(q_{1I}'' - q_{2I}''\right)}{h_{12}},\tag{20}$$

where the interfacial heat flux is,  $q_{kI}'' = -k_k \nabla T_k$ , and  $h_{12}$  is the generalized latent heat ( $h_{fg}$  for fluids in thermodynamic equilibrium). Also, we have from kinetic theory,

$$\Gamma_1 = K \left[ \frac{T_I - T_{sat} \left( p_g \right)}{T_{sat} \left( p_g \right)} \right], \tag{21}$$

where,  $K = \frac{\boldsymbol{b}h_{12}\mathbf{r}_2}{\sqrt{2\boldsymbol{p}RT_{sat}(p_2)}}$ , and  $\beta$  is an accommodation coefficient  $(0.0 \le \boldsymbol{b} \le 1.0)$ .

From an additional "body force" which accounts for the surface tension force, the liquid pressure at the interface is given by,

$$p_{1I} = p_{2I} - \mathbf{s}H(x, t)\underline{n}_{2},$$
and,  $\underline{n}_{1}p_{1I} + \underline{n}_{1} \Box \underline{\mathbf{t}}_{1I} = \underline{n}_{2}p_{2I} + \underline{n}_{2} \Box \underline{\mathbf{t}}_{2I} - \mathbf{s}H\underline{n}$  (22)

where  $\sigma$  is the surface tension of the interface, H is the curvature of the interface (only non-zero for elements that comprise the interface) and  $\underline{n}_2$  is the interface's normal vector.

The molar concentration of dissolved gas at the interface comes from an application of Henry's Law, which relates the interfacial concentration of a gas in the liquid to the partial pressure of the gas adjacent to the liquid:

$$\tilde{C} = \frac{p_{g_I}}{H_C} \tag{23}$$

where  $p_{g_I}$  is the partial pressure of the gas at the bubble's interface, and  $H_{\rm c}$  is the constant of Henry's Law.

## **EQUATION OF STATE**

## The Air Equation of State

The ideal gas equation of state, p = r(g-1)e, where  $\gamma = 1.4$ , has often been used for numerical evaluations during bubble growth and the initial collapse phase (a(t) >  $2a_0$ ), however, if we assume an adiabatic process, the pressure and temperature are less

than the initial room temperature, which is not realistic. In general, the numerical simulations of bubble collapse in the sonoluminescence regime depends strongly on the equation of state that is used to describe the air. Comparing the results obtained using an ideal gas ( $\gamma = 1.4$ ) and a high pressure equation of state (Moss et al. [10]), there is a (huge) difference between the maximum temperatures at the center of the bubble of about 735 eV ( $T_{max} = 875$  eV, for an ideal gas, and,  $T_{max} = 140$  eV using a high pressure equation of state). For an air bubble, during the final collapse phase, we may use the high-pressure equation of state given by Moss et al. [10]. This equation of state for air includes vibrational excitation, dissociation, and repulsive intermolecular potentials:

$$p = RT \mathbf{r} (1+m_D) (1+m) + \frac{E_c \mathbf{r}^0}{1-(3/n)} \left[ \left( \frac{\mathbf{r}}{\mathbf{r}^0} \right)^{(n/3)+1} - \left( \frac{\mathbf{r}}{\mathbf{r}^0} \right)^2 \right],$$

$$\mathbf{e} = \left[ \frac{5}{2} RT + \frac{R\Theta}{e^{\Theta/T-1}} \right] (1-m_D) + m_D RT_D +$$

$$\frac{3}{2} RT (2m_D) (1+m) + 2m_D R \sum_{i} m_i T_i + \frac{E_c}{(n/3)-1} \left[ \left( \frac{\mathbf{r}}{\mathbf{r}^0} \right)^{n/3} - \frac{n}{3} \left( \frac{\mathbf{r}}{\mathbf{r}^0} \right) \right] +$$

$$\frac{E_c}{(n/3)-1} \left[ \left( \frac{\mathbf{r}}{\mathbf{r}^0} \right)^{n/3} - \frac{n}{3} \left( \frac{\mathbf{r}}{\mathbf{r}^0} \right) \right] + E_c$$
(24)

where,  $m_{\rm K} = 0.5$  [tanh[7(T-0.9T<sub>K</sub>] + tanh [0.63]],  $\sum_{i=1}^{5} m_i$ , R = R/28.8, is the gas

vibrational contributions in the energy equation, respectively.

constant for air, and,  $m_D$ ,  $(0 \le m_D \le 1; T_D = 9.7 \text{ ev})$ ,  $m_i$   $(0 \le m_i \le 1; T_{1-5} = 14.5, 29.6, 47.4, 77.5, and 97.5 eV)$ , n (=9)  $\boldsymbol{r}^0$  (=1.113 g/cc),  $E_c$  (=2.52 x  $10^9$  erg/g), and,  $\Theta$  (=3340 K), are the dissociation of molecular nitrogen, the ionization, intermolecular potentials, the maximum density of the air, the binding energy of fully compressed air, and the

#### Noble Gas Equations of State

The noble gas equations of state (EOS) for argon and krypton were constructed from a combination of EOS table (Taleyarkhan [11]) and theory (Zel'dovichi [12]). The analytical equation of state for argon and krypton which fit the EOS table (Tale2arkhan [11]) are given by:

$$p = RT \mathbf{r} (1+m) + E_c \mathbf{r}^0 \exp \left[ \mathbf{a} \left( 1 - \left( \frac{\mathbf{r}^0}{\mathbf{r}} \right)^{0.3} \right) \right],$$

$$\mathbf{e} = \frac{3}{2} RT \Upsilon (\mathbf{j} + \overline{m}) + 2R \Upsilon \sum_{i} m_i T_i + E_c \left[ 1 + \exp \left\{ \mathbf{b} \left( 1 - \left( \frac{\mathbf{r}^0}{\mathbf{r}} \right)^{0.3} \right) \right\} \right]$$
(25)

where m is the average value of ionic charge discussed in Chapter 4, R = R/28.8 is the gas constant, the maximum densities,  $\boldsymbol{r}_s^0$ , for argon and krypton are 1770.7, 3090.0 kg/m<sup>3</sup>, respectively, the binding energies,  $E_c$ , for fully compressed argon and krypton are, respectively, 1.935 x  $10^5$  and 1.3265 x  $10^5$  J/kg. The numerical values for,  $\varphi$ ,  $\alpha$ ,  $\beta$ , and  $\Upsilon$  have been computed from:

$$\mathbf{j} = \sum_{i=0}^{2} c_{j} \left( T \times 10^{-4} \right)^{j}$$
,  $\Upsilon = 1$  for argon,  $\Upsilon = \varphi$  for krypton,

$$\boldsymbol{a} = \log \left( \frac{A_1}{E_c \boldsymbol{r}^0} \right) / \left[ 1 - \left( \frac{\boldsymbol{r}^0}{A_2} \right)^{0.3} \right]; \boldsymbol{b} = \log \left( \frac{A_3}{E_c} \right) / \left[ 1 - \left( \frac{\boldsymbol{r}^0}{A_2} \right)^{0.3} \right]$$

where the coefficients  $c_j$  and  $A_j$  for argon and krypton are presented in Table 1 and Table 2, respectively. Figures 1 and 2 show the energy and pressure isotherms calculated using the analytical equation described above and the data from EOS tables (Taleyarkhan [11]) for argon and krypton.

## The Water Equation of State

When an outward moving, large positive velocity, produced due to the reflection of strong shocks at the center of the bubble, arrives at the gas/liquid interface, the water

pressure near the interface becomes high enough to require the use of a nonlinear equation of state (Moss et al. [10]). For a water equation of state, we used a polynomial equation of state constructed by combining the predictions of several theoretical codes and experimental data (Ree [13]). The ionization process, and chemical equilibrium among dissociation products of water were all considered in this equation. An analytical form for the equation of state of water is given by:

$$p = (1 + \mathbf{z}) \left( \frac{G_1 + G_2 E + G_3 E^2 + G_4 E^3}{G_5 + G_6 E + G_7 E^2} \right) \text{ and, } G_i = \sum_{j=0}^{3} A_{ij} \mathbf{z}^j$$
 (26)

where p is in Tpa,  $\zeta = \rho/\rho^0$  - 1, E(tpa) =  $\epsilon \rho^0$ , and,  $\rho^0 = 0.998$  Mg/m³ (density at 298.5 K and standard pressure). The coefficients  $A_{ij}$  for in Eq. (26) are presented in Table 3. The range of applicability of Eq. (26) is  $0.025 \le T \le 10$  eV and  $0.998 < \rho < 40$  Mg/m³, and,  $p > 10^{-2}$  Mpa. Note that p and E in Eq. (26) are expressed in Tpa.

In addition to the above, we have developed an expression for the internal energy in terms of temperature and density. To derive this expression, we used the method proposed by Gurtman et al. [14]. Invoking a thermodynamic identity, we write:

$$\left(\frac{\partial \mathbf{e}}{\partial \mathbf{r}}\right)_{T} = \left(p - T\left(\frac{\partial p}{\partial T}\right)_{\mathbf{r}}\right) \mathbf{r}^{2} = g(\mathbf{r}).$$
(27)

For example, the compressional energy of a material is solely a function of its degree of compression. Integrating Eq. (27) yields:

$$\mathbf{e}(\mathbf{r},T) = \int_{\mathbf{r}_0}^{\mathbf{r}} g(\mathbf{r}) d\mathbf{r} + f(T)$$
 (28)

where the function f(T) represents the contribution due to the thermal motion of the molecules within the lattice. Assuming that the thermal contribution to the internal energy is linear with T, we obtain:

$$\left(\frac{\partial \mathbf{e}}{\partial T}\right)_{\mathbf{r}} = c_{v} = \text{constant.} \tag{29}$$

This assumption implies:

$$\boldsymbol{e} - \boldsymbol{e}_0 = c_v \left( T - T_0 \right) + \int_{\boldsymbol{r}_0}^{\boldsymbol{r}} g(\boldsymbol{r}) d\boldsymbol{r}$$
(30)

where the subscript 0 refer to the initial state of the material. Once forms of the compressional energy function  $g(\rho)$ , and a suitable value of  $c_V$ , are chosen, temperatures may be calculated using the density and internal energy, which are known. These quantities can be determined from the equation of state (EOS) data reported by Ree [13]. The assumption of a constant  $c_V$  requires that a compromise value be selected from the sparse EOS data. The  $c_V$  value chosen was 3.263 kJ/kg-K, to give a suitable fit of the EOS data. Numerical values for  $g(\rho)$  have been computed from the various combinations of high pressure isotherms from the relation:

$$g(\mathbf{r}) = \frac{p_i(\mathbf{r}) - (T_i/T_j)p_j}{1 - (T_i/T_j)},$$
(31)

where the subscripts denote particular isotherms. A polynomial fit to average values of these numerical data is given by:

$$g(\mathbf{r}) = \sum_{j=0}^{5} c_j \mathbf{r}^j. \tag{32}$$

Coefficients  $c_j$  are presented in Table 4. Figure 3 shows the internal energy as function of density for Rice and Walsh's data [15], which are for the water Hugoniot centered at  $20^{\circ}$ C and 1 *bar*. Using this equation of state for water and the data shown in Fig. 3(a), it is a straightforward matter to calculate the pressure, temperature, and speed of sound. These curves are plotted in Figs. 3(b-d). The Rice and Walsh data [15] are also shown for comparison to the present formulation.

These equations of state have been evaluated using a one-dimensional version of the conservation equations. The name of the computer code which was developed for this purpose was HYDRO-RPI [16].

Figures-4 show that there is good agreement with the available data [17], [18]. In addition, Figure-5 shows that there is good agreement between HYDRO-RPI and KYDNA, the HYDRO code developed at Lawrence Livermore Laboratory [19]. These comparisons verify the equations of state and serve as good benchmarks for HYDRO-RPI/3D.

## A NUMERICAL FORMULATION

The local, instantaneous generic balance equation for each phase can be expressed in conservative form as:

$$\underline{U}_{,t} + \underline{F}_{i,i}^{adv} = \underline{F}_{i,i}^{diff} + \underline{S} \tag{33}$$

where in three dimensions, the vector of the state variables,  $\underline{U}$ , is:

$$\underline{U} = \begin{cases} U_1 \\ U_2 \\ U_3 \\ U_4 \\ U_5 \end{cases} = \mathbf{r} \begin{cases} 1 \\ u \\ v \\ w \\ e^{tot} \end{cases} = \mathbf{r} \begin{cases} 1 \\ u_1 \\ u_2 \\ u_3 \\ e^{tot} \end{cases},$$
(34)

The advective flux in the *i*th-direction,  $\underline{F}_{i}^{adv}$ , is:

$$\underline{F}_{i}^{adv} = \mathbf{r}u_{i} \begin{cases} 1 \\ u_{1} \\ u_{2} \\ u_{3} \\ e^{tot} \end{cases} + p \begin{cases} 0 \\ \mathbf{d}_{1i} \\ \mathbf{d}_{2i} \\ \mathbf{d}_{3i} \\ u_{i} \end{cases},$$
(35)

The diffusive flux in the ith-direction,  $\underline{F}_{i}^{\textit{diff}}$  , is:

$$\underline{F}_{i}^{diff} = \begin{cases} 1 \\ \mathbf{t}_{1i} \\ \mathbf{t}_{2i} \\ \mathbf{t}_{3i} \\ \mathbf{t}_{1i}u_{j} \end{cases} + p \begin{cases} 0 \\ 0 \\ 0 \\ -q_{i} \end{cases},$$
(36)

and the source vector,  $\underline{S}$ , is:

$$\underline{S} = \mathbf{r} \begin{cases} 1 \\ b_1 \\ b_2 \\ b_3 \\ b_i u_i + r \end{cases}$$
(37)

The above vectors are written in terms of density,  $\rho$ , Cartesian velocity components,  $\underline{u} = \{u_1, u_2, u_3\}^T$ , total energy per unit mass,  $e^{tot} = e + |u|^2/2$ , where e is the internal energy per unit mass, thermodynamic pressure is p, the viscous-stress tensor is  $\underline{t} = [t_{ij}]$ , heat flux vector is  $\underline{q} = \{q_1, q_2, q_3\}^T$ , the body force vector per unit mass  $\underline{b} = \{b_1, b_2, b_3\}^T$ , and the heat source per unit mass is  $r = rq^m$ . Also,  $d_{ij}$  is the Kronecker delta (i.e.,  $d_{ij=1}$  for, i = j and  $d_{ij} = 0$  for  $i \neq j$ ), a comma represents partial differentiation and the summation convention is used throughout. As noted previously, we consider as constitutive relations a linear deformation law for the stress tensor and the Fourier's law for heat conduction. That is,

$$\boldsymbol{t}_{ij} = \boldsymbol{m} \left( u_{i,j} + u_{j,i} \right) + \boldsymbol{I} u_{k,k} \boldsymbol{d}_{ij} \tag{38}$$

$$q_i = -kT_{,i} \tag{39}$$

For convenience, we define the constant  $x = \lambda + 2\mu$ . Using any set of variables,  $\underline{Y}$ , it is possible to rewrite Eq. (33) in quasi-linear form as:

$$\underline{\underline{A}}_{0}\underline{Y}_{,t} + \underline{\underline{A}}_{i}\underline{Y}_{,i} = \left(\underline{\underline{K}}_{ij}\underline{Y}_{,j}\right)_{,i} + \underline{\underline{S}}$$

$$\tag{40}$$

where,  $\underline{\underline{A}}_0 = \underline{U}$ ,  $\underline{\underline{A}}_i = \underline{F}_{i,Y}^{adv}$  is the  $i_{th}$  Euler Jacobian matrix, and,  $\underline{\underline{K}}_{ij}$  is the

diffusivity matrix, where,  $\underline{\underline{K}}_{ij}Y$ ,  $_{j}=\underline{F}_{i}^{diff}$ .

In HYDRO-RPI/3D the SUPG stabilization method was applied with linearly interpolated pressure-primitive variables.

$$\underline{Y} = \begin{cases} Y_1 \\ Y_2 \\ Y_3 \\ Y_4 \\ Y_5 \end{cases} = \begin{cases} p \\ u_1 \\ u_2 \\ u_3 \\ T \end{cases}$$
(41)

The matrix  $\underline{\underline{A}}_0$  can be written as:

$$\underline{\underline{A}}_{0} = \frac{\partial}{\partial [p, u_{1}, u_{2}, u_{3}, T]} \begin{Bmatrix} \mathbf{r} \\ \mathbf{r}u_{1} \\ \mathbf{r}u_{2} \\ \mathbf{r}u_{3} \\ \mathbf{r}e^{tot} \end{Bmatrix} = \begin{bmatrix} \frac{\partial \mathbf{r}}{\partial p} & 0 & 0 & 0 & \frac{\partial \mathbf{r}}{\partial T} \\ u_{1} \frac{\partial \mathbf{r}}{\partial p} & \mathbf{r} & 0 & 0 & u_{1} \frac{\partial \mathbf{r}}{\partial T} \\ u_{2} \frac{\partial \mathbf{r}}{\partial p} & 0 & \mathbf{r} & 0 & u_{2} \frac{\partial \mathbf{r}}{\partial T} \\ u_{3} \frac{\partial \mathbf{r}}{\partial p} & 0 & 0 & \mathbf{r} & u_{3} \frac{\partial \mathbf{r}}{\partial T} \\ \frac{\partial \mathbf{r}e^{tot}}{\partial p} & \mathbf{r}u_{1} & \mathbf{r}u_{2} & \mathbf{r}u_{3} & \frac{\partial \mathbf{r}e^{tot}}{\partial T} \end{bmatrix}$$
(42)

The Euler Jacobians with respect to  $\underline{Y}$ ,  $\underline{\underline{A}}_i = \underline{F}_{i,Y}^{adv}$ , are given by:

$$\underline{\underline{A}}_{1} = \frac{\partial}{\partial [p, u_{1}, u_{2}, u_{3}, T]} \begin{cases} \mathbf{r}u_{1} \\ \mathbf{r}u_{1}^{2} + p \\ \mathbf{r}u_{1}u_{2} \\ \mathbf{r}u_{1}u_{3} \\ \mathbf{r}u_{1}e^{tot} + pu_{1} \end{cases}$$

$$=\begin{bmatrix} u_{1}\frac{\partial \mathbf{r}}{\partial p} & \mathbf{r} & 0 & 0 & u_{1}\frac{\partial \mathbf{r}}{\partial T} \\ u_{1}^{2}\frac{\partial \mathbf{r}}{\partial p} + 1 & 2\mathbf{r}u_{1} & 0 & 0 & u_{1}^{2}\frac{\partial \mathbf{r}}{\partial T} \\ u_{1}u_{2}\frac{\partial \mathbf{r}}{\partial p} & \mathbf{r}u_{2} & \mathbf{r}u_{1} & 0 & u_{1}u_{2}\frac{\partial \mathbf{r}}{\partial T} \\ u_{1}u_{3}\frac{\partial \mathbf{r}}{\partial p} & \mathbf{r}u_{3} & 0 & \mathbf{r}u_{1} & u_{1}u_{3}\frac{\partial \mathbf{r}}{\partial T} \\ u_{1}\left(\frac{\partial \mathbf{r}e^{tot}}{\partial p} + 1\right) & \mathbf{r}e^{tot} + p & \mathbf{r}u_{1}u_{2} & \mathbf{r}u_{1}u_{3} & u_{1}\frac{\partial \mathbf{r}e^{tot}}{\partial T} \end{bmatrix}$$

$$(43)$$

$$\underline{\underline{A}}_{2} = \frac{\partial}{\partial [p, u_{1}, u_{2}, u_{3}, T]} \begin{Bmatrix} \mathbf{r}u_{1} \\ \mathbf{r}u_{2}u_{2} \\ \mathbf{r}u_{2}^{2} + p \\ \mathbf{r}u_{2}u_{3} \\ \mathbf{r}u_{2}e^{tot} + pu_{2} \end{Bmatrix}$$

$$\begin{bmatrix}
u_{2}\frac{\partial \mathbf{r}}{\partial p} & 0 & \mathbf{r} & 0 & u_{2}\frac{\partial \mathbf{r}}{\partial T} \\
u_{1}u_{2}\frac{\partial \mathbf{r}}{\partial p} & \mathbf{r}u_{2} & \mathbf{r}u_{1} & 0 & u_{1}u_{2}\frac{\partial \mathbf{r}}{\partial T} \\
u_{2}\frac{\partial \mathbf{r}}{\partial p} & 2\mathbf{r}u_{2}+1 & 0 & 0 & u_{2}^{2}\frac{\partial \mathbf{r}}{\partial T} \\
u_{2}u_{3}\frac{\partial \mathbf{r}}{\partial p} & 0 & \mathbf{r}u_{3} & \mathbf{r}u_{2} & u_{2}u_{3}\frac{\partial \mathbf{r}}{\partial T} \\
u_{2}\left(\frac{\partial \mathbf{r}e^{tot}}{\partial p}+1\right) & \mathbf{r}u_{1}u_{2} & \mathbf{r}e^{tot}+p & \mathbf{r}u_{2}u_{3} & u_{2}\frac{\partial \mathbf{r}e^{tot}}{\partial T}
\end{bmatrix}$$
(44)

and,

$$\underline{\underline{A}}_{3} = \frac{\partial}{\partial [p, u_{1}, u_{2}, u_{3}, T]} \begin{cases} \mathbf{r}u_{3} \\ \mathbf{r}u_{1}u_{3} \\ \mathbf{r}u_{2}u_{3} \\ \mathbf{r}u_{3}^{2} + p \\ \mathbf{r}u_{3}e^{tot} + pu_{3} \end{cases}$$

$$=\begin{bmatrix} u_{3}\frac{\partial \mathbf{r}}{\partial p} & 0 & 0 & \mathbf{r} & u_{3}\frac{\partial \mathbf{r}}{\partial T} \\ u_{1}u_{3}\frac{\partial \mathbf{r}}{\partial p} & \mathbf{r}u_{3} & 0 & \mathbf{r}u_{1} & u_{1}u_{3}\frac{\partial \mathbf{r}}{\partial T} \\ u_{2}u_{3}\frac{\partial \mathbf{r}}{\partial p} & 0 & \mathbf{r}u_{3} & \mathbf{r}u_{2} & u_{2}^{2}\frac{\partial \mathbf{r}}{\partial T} \\ u_{3}^{2}\frac{\partial \mathbf{r}}{\partial p} & 0 & 2\mathbf{r}u_{3} & 0 & u_{3}^{2}\frac{\partial \mathbf{r}}{\partial T} \\ u_{3}\left(\frac{\partial \mathbf{r}e^{tot}}{\partial p}+1\right) & \mathbf{r}u_{1}u_{3} & \mathbf{r}u_{2}u_{3} & \mathbf{r}e^{tot}+p & u_{3}\frac{\partial \mathbf{r}e^{tot}}{\partial T} \end{bmatrix}$$

$$(45)$$

The equation of states discussed in Section 3 have been used to calculate the partial derivatives in the matrices. The diffusivity coefficient matrices,  $\underline{\underline{K}}_{ij}$ , where

$$\underline{\underline{K}}_{ij}\underline{Y}$$
,  $j = \underline{F}_i^{diff}$ , are:

$$\underline{K}_{11} = \begin{bmatrix} 0 & 0 & 0 & 0 & 0 \\ 0 & x & 0 & 0 & 0 \\ 0 & 0 & \mathbf{m} & 0 & 0 \\ 0 & 0 & 0 & \mathbf{m} & 0 \\ 0 & xu_1 & \mathbf{m}u_2 & \mathbf{m}u_3 & k \end{bmatrix}, \quad \underline{K}_{12} = \begin{bmatrix} 0 & 0 & 0 & 0 & 0 & 0 \\ 0 & 0 & \mathbf{l} & 0 & 0 & 0 \\ 0 & \mathbf{m} & 0 & 0 & 0 \\ 0 & \mathbf{m}u_2 & \mathbf{l}u_2 & 0 & 0 \end{bmatrix}, \underline{K}_{13} = \begin{bmatrix} 0 & 0 & 0 & 0 & 0 & 0 \\ 0 & 0 & 0 & \mathbf{l} & 0 \\ 0 & \mathbf{m} & 0 & \mathbf{m} & 0 \\ 0 & \mathbf{m}u_3 & 0 & \mathbf{l}u_1 & 0 \end{bmatrix}$$

$$\underline{\underline{K}}_{21} = \begin{bmatrix} 0 & 0 & 0 & 0 & 0 & 0 \\ 0 & 0 & \mathbf{m} & 0 & 0 & 0 \\ 0 & \mathbf{l} & 0 & 0 & 0 & 0 \\ 0 & \mathbf{l} u_2 & \mathbf{m} u_1 & 0 & 0 \end{bmatrix}, \quad \underline{\underline{K}}_{22} = \begin{bmatrix} 0 & 0 & 0 & 0 & 0 & 0 \\ 0 & \mathbf{m} & 0 & 0 & 0 & 0 \\ 0 & 0 & 0 & \mathbf{m} & 0 & 0 \\ 0 & \mathbf{m} u_1 & x u_2 & \mathbf{m} u_3 & k \end{bmatrix}, \quad \underline{\underline{K}}_{23} = \begin{bmatrix} 0 & 0 & 0 & 0 & 0 & 0 \\ 0 & 0 & 0 & \mathbf{l} & 0 & 0 \\ 0 & 0 & \mathbf{m} & 0 & 0 & 0 \\ 0 & 0 & 0 & \mathbf{m} & 0 & 0 \\ 0 & 0 & 0 & \mathbf{m} & 0 & 0 \\ 0 & 0 & 0 & \mathbf{m} & 0 & 0 \\ 0 & 0 & 0 & \mathbf{m} & 0 & 0 \\ 0 & 0 & 0 & \mathbf{m} & 0 & 0 \\ 0 & 0 & 0 & \mathbf{m} & 0 & 0 \\ 0 & 0 & 0 & \mathbf{m} & 0 & 0 \\ 0 & 0 & 0 & \mathbf{m} & 0 & 0 \\ 0 & 0 & 0 & \mathbf{m} & 0 & 0 \\ 0 & 0 & 0 & \mathbf{m} & 0 & 0 \\ 0 & 0 & 0 & \mathbf{m} & 0 & 0 \\ 0 & 0 & 0 & \mathbf{m} & 0 & 0 \\ 0 & 0 & 0 & \mathbf{m} & 0 & 0 \\ 0 & 0 & \mathbf{m} & 0 & 0 & 0 \\ 0 & \mathbf{m} & 0 & 0 & 0 \\ 0 & \mathbf{m} & 0 & 0 & 0 \\ 0 & \mathbf{m} & 0 & 0 & 0 \\ 0 & \mathbf{m} & 0 & x & 0 \\ 0 & \mathbf{m} & 0 &$$

and.

$$\underline{F}_{1}^{diff} = \underline{K}_{1j}\underline{Y}, j = \underline{K}_{11} \begin{cases} \partial p/\partial x_{1} \\ \partial u_{1}/\partial x_{1} \\ \partial u_{2}/\partial x_{1} \\ \partial u_{3}/\partial x_{1} \\ \partial T/\partial x_{1} \end{cases} + \underline{K}_{12} \begin{cases} \partial p/\partial x_{2} \\ \partial u_{1}/\partial x_{2} \\ \partial u_{2}/\partial x_{2} \\ \partial T/\partial x_{2} \end{cases} + \underline{K}_{13} \begin{cases} \partial p/\partial x_{3} \\ \partial u_{1}/\partial x_{3} \\ \partial u_{2}/\partial x_{3} \\ \partial U_{2}/\partial x_{3} \\ \partial U_{3}/\partial x_{3} \\ \partial T/\partial x_{3} \end{cases}$$

$$\underline{F}_{2}^{diff} = \underline{K}_{2j}\underline{Y}, j = \underline{K}_{21} \begin{cases} \partial p/\partial x_{1} \\ \partial u_{1}/\partial x_{1} \\ \partial u_{2}/\partial x_{1} \\ \partial T/\partial x_{1} \end{cases} + \underline{K}_{22} \begin{cases} \partial p/\partial x_{2} \\ \partial u_{1}/\partial x_{2} \\ \partial u_{2}/\partial x_{2} \\ \partial T/\partial x_{2} \end{cases} + \underline{K}_{23} \begin{cases} \partial p/\partial x_{3} \\ \partial u_{1}/\partial x_{3} \\ \partial u_{2}/\partial x_{3} \\ \partial U_{2}/\partial x_{3} \\ \partial U_{2}/\partial x_{3} \\ \partial U_{2}/\partial x_{3} \end{cases}$$

$$\underline{F}_{3}^{diff} = \underline{K}_{3j}\underline{Y}, j = \underline{K}_{31} \begin{cases} \partial p/\partial x_{1} \\ \partial u_{1}/\partial x_{1} \\ \partial u_{2}/\partial x_{1} \\ \partial u_{2}/\partial x_{1} \\ \partial U_{2}/\partial x_{2} \end{cases} + \underline{K}_{32} \begin{cases} \partial p/\partial x_{2} \\ \partial u_{1}/\partial x_{2} \\ \partial u_{2}/\partial x_{2} \\ \partial u_{2}/\partial x_{2} \\ \partial u_{2}/\partial x_{2} \end{cases} + \underline{K}_{33} \begin{cases} \partial p/\partial x_{3} \\ \partial U_{1}/\partial x_{3} \\ \partial U_{1}/\partial x_{3} \\ \partial U_{2}/\partial x_{3} \\ \partial U_{2}/\partial x_{3} \end{cases}$$

$$\underline{F}_{3}^{diff} = \underline{K}_{3j}\underline{Y}, j = \underline{K}_{31} \begin{cases} \partial p/\partial x_{1} \\ \partial u_{2}/\partial x_{1} \\ \partial u_{2}/\partial x_{1} \\ \partial U_{2}/\partial x_{2} \end{cases} + \underline{K}_{32} \begin{cases} \partial p/\partial x_{2} \\ \partial u_{2}/\partial x_{2} \\ \partial u_{2}/\partial x_{2} \\ \partial u_{2}/\partial x_{2} \end{cases} + \underline{K}_{33} \begin{cases} \partial p/\partial x_{3} \\ \partial u_{1}/\partial x_{3} \\ \partial u_{2}/\partial x_{3} \\ \partial u_{1}/\partial x_{3} \end{cases}$$

$$\underline{F}_{3}^{diff} = \underline{K}_{3j}\underline{Y}, j = \underline{K}_{31} \begin{cases} \partial p/\partial x_{1} \\ \partial u_{2}/\partial x_{1} \\ \partial u_{2}/\partial x_{1} \\ \partial u_{3}/\partial x_{2} \\ \partial u_{2}/\partial x_{2} \end{cases} + \underline{K}_{33} \begin{cases} \partial p/\partial x_{2} \\ \partial u_{2}/\partial x_{2} \\ \partial u_{3}/\partial x_{3} \\ \partial u_{2}/\partial x_{3} \end{cases}$$

$$\underline{F}_{3}^{diff} = \underline{K}_{3j}\underline{Y}, j = \underline{K}_{31} \begin{cases} \partial p/\partial x_{1} \\ \partial u_{2}/\partial x_{1} \\ \partial u_{3}/\partial x_{1} \\ \partial u_{3}/\partial x_{2} \\ \partial u_{3}/\partial x_{2} \end{cases}$$

$$\underline{F}_{3}^{diff} = \underline{K}_{3j}\underline{Y}, j = \underline{K}_{31} \begin{cases} \partial p/\partial x_{1} \\ \partial u_{2}/\partial x_{1} \\ \partial u_{3}/\partial x_{1} \\ \partial u_{3}/\partial x_{2} \\ \partial u_{3}/\partial x_{2} \end{cases}$$

$$\underline{F}_{3}^{diff} = \underline{K}_{3j}\underline{Y}, j = \underline{K}_{31} \begin{cases} \partial p/\partial x_{1} \\ \partial u_{2}/\partial x_{1} \\ \partial u_{3}/\partial x_{2} \\ \partial u_{3}/\partial x_{3} \\ \partial$$

Here, we consider the system of governing equations arising when the evolution of the interface function, defined in Section 2, is appended to the local, instantaneous generic balance equation. For convenience,  $\underline{U}$  and  $\underline{Y}$  are repeated here:

$$\underline{U} = \begin{cases} U_1 \\ U_2 \\ U_3 \\ U_4 \\ U_5 \\ U_6 \end{cases} = \mathbf{r} \begin{cases} 1 \\ u \\ v \\ w \\ e^{tot} \\ \Phi/\mathbf{r} \end{cases} = \mathbf{r} \begin{cases} 1 \\ u_1 \\ u_2 \\ u_3 \\ e^{tot} \\ \Phi/\mathbf{r} \end{cases}, \qquad \underline{Y} = \begin{cases} Y_1 \\ Y_2 \\ Y_3 \\ Y_4 \\ Y_5 \\ Y_6 \end{cases} = \begin{cases} p \\ u_1 \\ u_2 \\ u_3 \\ T \\ \Phi \end{cases}, \tag{48}$$

The matrix tensor  $\underline{\underline{A}}_0$  can be written as:

$$\underline{\underline{A}}_{0} = \begin{bmatrix} \frac{\partial \mathbf{r}}{\partial p} & 0 & 0 & 0 & \frac{\partial \mathbf{r}}{\partial T} & 0 \\ u_{1} \frac{\partial \mathbf{r}}{\partial p} & \mathbf{r} & 0 & 0 & u_{1} \frac{\partial \mathbf{r}}{\partial T} & 0 \\ u_{2} \frac{\partial \mathbf{r}}{\partial p} & 0 & \mathbf{r} & 0 & u_{2} \frac{\partial \mathbf{r}}{\partial T} & 0 \\ u_{3} \frac{\partial \mathbf{r}}{\partial p} & 0 & 0 & \mathbf{r} & u_{3} \frac{\partial \mathbf{r}}{\partial T} & 0 \\ \frac{\partial \mathbf{r}e^{tot}}{\partial \mathbf{r}} & \mathbf{r}u_{1} & \mathbf{r}u_{2} & \mathbf{r}u_{3} & \frac{\partial \mathbf{r}e^{tot}}{\partial T} & 0 \\ 0 & 0 & 0 & 0 & 0 & 1 \end{bmatrix}$$

$$(49)$$

The advective Jacobian matrice,  $\underline{\underline{A}}_i = \underline{F}_{i,Y}^{adv}$ , are given by:

$$\underline{\underline{A}}_{1} = \begin{bmatrix} u_{1}\frac{\partial \mathbf{r}}{\partial p} & \mathbf{r} & 0 & 0 & u_{1}\frac{\partial \mathbf{r}}{\partial T} & 0 \\ u_{1}^{2}\frac{\partial \mathbf{r}}{\partial p} & 2\mathbf{r}u_{1} & 0 & 0 & u_{1}^{2}\frac{\partial \mathbf{r}}{\partial T} & 0 \\ u_{1}u_{2}\frac{\partial \mathbf{r}}{\partial p} & \mathbf{r}u_{2} & \mathbf{r}u_{1} & 0 & u_{1}u_{2}\frac{\partial \mathbf{r}}{\partial T} & 0 \\ u_{1}u_{3}\frac{\partial \mathbf{r}}{\partial p} & \mathbf{r}u_{3} & 0 & \mathbf{r}u_{1} & u_{1}u_{3}\frac{\partial \mathbf{r}}{\partial p} & 0 \\ u_{1}\left(\frac{\partial \mathbf{r}e^{tot}}{\partial p}+1\right) & \mathbf{r}e^{tot}+p & \mathbf{r}u_{1}u_{2} & \mathbf{r}u_{1}u_{3} & u_{1}\frac{\partial \mathbf{r}e^{tot}}{\partial T} & 0 \\ 0 & 0 & 0 & 0 & 0 & u_{I} \end{bmatrix}$$

$$u_2^2 \frac{\partial \mathbf{r}}{\partial p} \qquad 2\mathbf{r}u_2 + 1 \qquad 0 \qquad 0 \qquad u_2^2 \frac{\partial \mathbf{r}}{\partial T} \qquad 0$$

 $\underline{\underline{A}}_{2} = \begin{bmatrix} u_{2}\frac{\partial \mathbf{r}}{\partial p} & 0 & \mathbf{r} & 0 & u_{2}\frac{\partial \mathbf{r}}{\partial T} & 0 \\ u_{1}u_{2}\frac{\partial \mathbf{r}}{\partial p} & \mathbf{r}u_{2} & \mathbf{r}u_{1} & 0 & u_{1}u_{2}\frac{\partial \mathbf{r}}{\partial T} & 0 \\ u_{2}^{2}\frac{\partial \mathbf{r}}{\partial p} & 2\mathbf{r}u_{2}+1 & 0 & 0 & u_{2}^{2}\frac{\partial \mathbf{r}}{\partial T} & 0 \\ u_{2}u_{3}\frac{\partial \mathbf{r}}{\partial p} & 0 & \mathbf{r}u_{3} & \mathbf{r}u_{2} & u_{2}u_{3}\frac{\partial \mathbf{r}}{\partial T} & 0 \\ u_{2}\left(\frac{\partial \mathbf{r}e^{tot}}{\partial p}+1\right) & \mathbf{r}u_{1}u_{2} & \mathbf{r}e^{tot}+p & \mathbf{r}u_{2}u_{3} & u_{2}\frac{\partial \mathbf{r}e^{tot}}{\partial T} & 0 \\ 0 & 0 & 0 & 0 & v_{I} \end{bmatrix}$ 

(51)

(50)

$$\underline{\underline{A}}_{3} = \begin{bmatrix} u_{3}\frac{\partial \mathbf{r}}{\partial p} & 0 & 0 & \mathbf{r} & u_{3}\frac{\partial \mathbf{r}}{\partial T} & 0 \\ u_{1}u_{3}\frac{\partial \mathbf{r}}{\partial p} & \mathbf{r}u_{3} & 0 & \mathbf{r}u_{1} & u_{1}u_{3}\frac{\partial \mathbf{r}}{\partial T} & 0 \\ u_{2}u_{3}\frac{\partial \mathbf{r}}{\partial p} & 0 & \mathbf{r}u_{3} & \mathbf{r}u_{2} & u_{2}^{2}\frac{\partial \mathbf{r}}{\partial T} & 0 \\ u_{3}^{2}\frac{\partial \mathbf{r}}{\partial p} & 0 & 2\mathbf{r}u_{3} & 0 & u_{3}^{2}\frac{\partial \mathbf{r}}{\partial p} & 0 \\ u_{3}\left(\frac{\partial \mathbf{r}e^{tot}}{\partial p}+1\right) \mathbf{r}u_{1}u_{3} & \mathbf{r}u_{2}u_{3} & \mathbf{r}e^{tot}+p & u_{3}\frac{\partial \mathbf{r}e^{tot}}{\partial T} & 0 \\ 0 & 0 & 0 & 0 & w_{I} \end{bmatrix}$$

$$(52)$$

The diffusivity coefficient matrices,  $\underline{\underline{K}}_{ij}$ , where  $\underline{\underline{K}}_{ij}\underline{Y}$ ,  $\underline{j} = \underline{F}_i^{diff}$ , are:

$$\underline{\underline{K}}_{33} = \begin{bmatrix} 0 & 0 & 0 & 0 & 0 & 0 \\ 0 & \mathbf{m} & 0 & 0 & 0 & 0 \\ 0 & \mathbf{m} & 0 & 0 & 0 & 0 \\ 0 & \mathbf{m} & 0 & x & 0 & 0 \\ 0 & \mathbf{m}u_1 & \mathbf{m}u_2 & xu_3 & k & 0 \\ 0 & 0 & 0 & 0 & 0 & 0 \end{bmatrix} . \tag{53}$$

For the discussion that follows, it is helpful to define the quasi-linear operator of Eq. (40)

as:

$$\underline{\underline{L}} \equiv \underline{\underline{A}}_0 \frac{\partial}{\partial t} + \underline{\underline{A}}_i \frac{\partial}{\partial x_i} - \frac{\partial}{\partial x_i} \left( \underline{\underline{K}}_{ij} \frac{\partial}{\partial x_i} \right)$$
 (54)

from which L can be naturally decomposed into time, advective, and diffusive components

$$\underline{\underline{L}} = \underline{\underline{L}}_t + \underline{\underline{L}}_{adv} + \underline{\underline{L}}_{diff}. \tag{55}$$

Using this, we can rewrite Eq. (40) as simply,  $\underline{\underline{L}}\underline{\underline{Y}} = \underline{\underline{S}}$ .

To help proceed with the finite element discretization of the local, instantaneous generic balance equation, Eq. (40), we can define some notation. First let  $\Omega$  represent the closure of the

physical spatial domain (i.e.,  $\Omega \cup \Gamma$  where  $\Gamma$  is the boundary). Next,  $\Omega$  is discretized into  $n_{el}$  finite elements,  $\Omega^e$ . To derive the so-called weak form of Eq. (40), the entire equation may be dotted from the left by a vector of weight functions,  $\underline{W}$ , and integrated over the spatial domain. Integration by parts is then performed to move the spatial derivatives onto the weight functions (reducing the continuity requirements). This process leads to an integral equation (often referred to as the weak form), in which we seek to find  $\underline{Y}$  such that,

$$0 = \int_{\Omega} \left( \underline{W} \cdot \underline{\underline{A}}_{0} \underline{Y},_{t} - \underline{W},_{i} \cdot \underline{F}^{adv} + \underline{W},_{i} \cdot \underline{F}^{diff} - \underline{W} \cdot \underline{S} \right) d\Omega - \int_{\Gamma} \underline{W} \cdot \left( \underline{F}_{i}^{adv} + \underline{F}_{i}^{diff} \right) d\Gamma$$

$$+ \sum_{e=1}^{n_{el}} \int_{\Omega^{e}} \underline{L}^{T} \underline{W} \cdot \mathbf{t} \left( \underline{\underline{L}} \underline{Y} - \underline{S} \right) d\Omega^{e}$$
(56)

The first line of Eq. (56) contains the Galerkin approximation (interior and boundary) and the second line contains a least-squares stabilization. The SUPG stabilization is obtained by replacing  $\underline{\underline{L}}^T$  by  $\underline{\underline{L}}_{adv}^T$ .

To develop a numerical method, the weight functions ( $\underline{W}$ ), the solution variables ( $\underline{Y}$ ), and their time derivatives ( $\underline{Y}$ ,  $_t$ ), are expanded in terms of basis functions using (typically) piecewise polynomials. The integrals in Eq. (56) are then evaluated using Gauss quadrature, resulting in a system of non-linear ordinary differential equations which can be written as,

$$\underline{MY}_{,t} = \underline{R(Y)} \tag{57}$$

where  $\underline{Y}$  is the vector of the solution at discrete points (interpolated through the space by the basis functions), and  $(\underline{Y},_t)$  are the time derivative values at the same points. An implicit, second order accurate family of time integrators has been used for application to this problem. The method results in a non-linear matrix problem that is solved in a predictor-corrector format yielding successive linear problems. Each linear problem is then solved using a Matrix-Free Generalized Minimal Residual (MF-GMRES) solution technique with a block diagonal preconditioner which was developed by Johan et al. [18]. Convergence of the non-linear problem is confirmed before moving to the next step.

# LOCATION OF INTERFACE

The treatment of the interface is crucial for the application of right constitutive laws to each phase. We use a fixed mesh and a transport equation for the position of interface Eq. (14). Based on the values of phase indicator function,  $\Phi$ , at the nodes, an example for prediction of the interface location is shown in Fig. 6.

Let us assume that an intermediate value marks the interface (i.e.,  $\Phi=0.5$ ). Therefore there is no interface between the two nodes if both indicator functions greater or less than 0.5, (i.e.,  $\Phi_1$  and  $\Phi_3$ ). Except for these conditions, the point indicating the interface between two nodes is calculated by linear interpolation, for example:

$$x_{I_1} = \frac{0.5 - c_{x0}}{c_{x1}},\tag{58}$$

where,  $c_{x1} = \frac{\Phi_2^e - \Phi_1^e}{x_2 - x_1}$ , and,  $c_{x0} = \Phi_1^e - c_{x1}x_1$ . The  $y_{I_1}$  and  $z_{I_1}$  are calculated in the same

manner as above.

It should be noted that the values of the two-phase state variables are also given by interpolation of the FEM results. For example, the two-phase density comes from,

$$\overline{r} = \frac{m_{\ell} - m_{V}}{V_{\ell} + V_{V}}$$

where, for example, the  $V_\ell$  comes from a linear interpolation using Eq. (58). This approach is different from standard VOF formulations which smear the interface.

#### NUMERICAL SIMULATION OF A SINGLE BUBBLE:

The following cases have been simulated using the numerical treatment described in the previous sections

- 1. Motion of a single bubble in pure advection flow
- 2. Rising of single bubble in stagnant pool

These tests verify that our VOF method can solve 2D problems as required at this stage of the grant.

#### **PRELIMINARY RESULTS:**

1.Motion of a single bubble in pure advection flow

This is the simulation of a bubble in a pure convection channel. The bubble is initially located at the bottom of the channel as shown in the Figure.7. Then the fluid enters the channel with a uniform flow of 1m/sec in vertical direction (x-direction). In this simulation, the buoyancy effect on the bubble is not considered, so it is a pure convection flow. At the channel inlet, the uniform velocity of the flow is prescribed and at the exit of the channel constant pressure boundary condition is applied. The channel is considered periodic in the sides (y-direction), and the channel walls (z-direction) are prescribed with a zero velocity normal to the wall, and with zero traction.

The grid applied has 40 elements in x-direction, 16 elements in y-direction and a single element in z-direction. The time step chosen is 1.25 sec. In the absence of the buoyancy force, the bubble should move along the channel with the speed of the fluid. Figure.8 and Figure.9 shows the position of the bubble in the channel after 20 and 40 time steps respectively. As expected the bubble is moving with the velocity of the fluid, which clearly reflects in the figures, as the bubble is advanced by 10 elements in 20 time steps, and by 20 elements in 40 time steps, indicating that the bubble is moving with a velocity of 1m/sec.

## 2. Rising of single bubble in stagnant pool

This is modeling of the bubble motion due to buoyancy in a stagnant pool of fluid. Initially the bubble is at rest at the bottom of the pool as shown in the Figure.10. In this case a gravitational force of  $0.03\text{m/sec}^2$  is applied in the negative y-direction. Due to the buoyancy

force acting on the bubble, the bubble should rise through the stagnant poll pushing the fluid aside.

A zero velocity boundary condition is applied at the bottom of the pool, and a constant pressure boundary condition is assigned to the pool surface. The pool is made periodic in both x, and z-directions. A hydrostatic pressure profile is defined as an initial condition for the entire pool domain. The grid used has 80 elements in y-direction, and 64 elements in x-direction and a single element in z-direction. A time step of 0.25 sec is used for the results presented here. The position of the bubble after 20 time steps and 40 time steps is shown in the Figures 11 and 12. From the figures it is clear that the bubble started to rise under the effect of buoyancy. As the bubble raises though the pool, the fluid surrounding the bubble gets pushed up and around the sides as shown by the fluid velocity vectors in the figures.

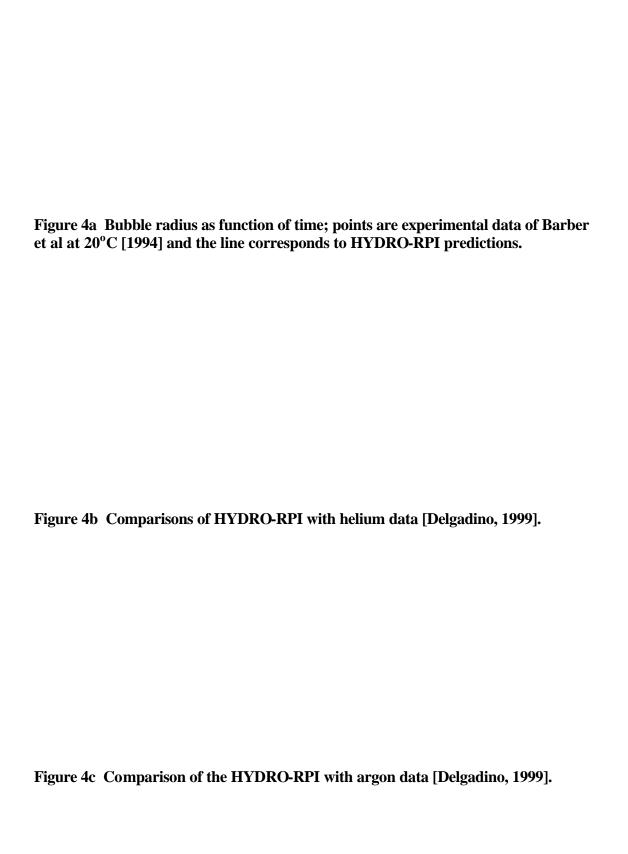
#### **CONCLUSIONS**

With the equation of state well defined and the 2D VOF results validated we are now prepared to turn our attention to 3D bubble dynamics as require for the simulation of sonoluminescense. The VOF results while encouraging will also be compared to level set methods which are expected to more easily track the discontinuous interface between the two phases.

#### REFERENCES

- [1] C.W. Hirt, A.A. Amsden and J.L. Cook, "Arbitrary Lagrangian-Eulerian computing method of all speeds", *J. Comput. Phys.* **14**, 227 (1974).
- [2] J. Donea, "Arbitrary Lagrangian-Eurlerian finite element methods", *Comput. Methods Transient Anal.* **1**, 473-516 (1983).
- [3] T.J.R. Hughes, W.K. Liu and T.K. Zimmerman, "Lagrangian-Eulerianfinite element formulation for incompressible viscous flows", *U.S. Japan Seminar on Interdisciplinary Finite Element Analysis*, Cornell Univ., Ithaca, NY, August 7-11 (1978).
- [4] W.K. Liu, T. Belytshko and H. Chang, "An arbitrary Lagrangian-Eulerian finite element method for path-dependant materials", *Comput. Methods Appl. Mech. Engrg.* **58**, 227-245 (1986).
- [5] T.E. Tezduyar, M. Behr and J. Liou, "A new strategy for finite element computations involving moving boundaries and interface-the deforming-spatial-domain/space-time procedure. The concept and preliminary tests", *Comput. Methods Appl. Mech. Engrg.* **94**, 339-351 (1992).
- [6] T.E. Tezduyar, M. Behr, S. Mittal and J. Liou, "A new strategy for finite element computations involving moving boundaries and interfaces-the deforming-spatial-domain/space-time procedures: II Computation of free-surface flows, two-liquid flows, and flows with drifting cylinders", *Comput. Methods Appl. Mech. Engrg.* **94**, 353-371 (1992).
- [7] T.J.R. Hughes, L.P. Franca, and M. Mallet, "A new finite element formulation for fluid dynamics-VI. Convergence analysis of the generalized SUPG formulation for linear time-dependent multidimensional advective-diffusive systems", *Comput. Methods Appl. Mech. Engrg.* **63**, 97-112 (1987).
- [8] T.J.R. Hughes, L.P. Franca, and G.M. Hulbert, "A new finite element formulation for fluid dynamics-VIII. The Galerkin/Least-squares method for advective-diffusive equations", *Comput. Methods Appl. Mech. Engrg.* **73**, 173-189 (1989).
- [9] L.P. Franca and T.J.R. Hughes, "Convergence analyses of Galerkin/Least-squares methods for symmetric advective-diffusive forms of the Stokes and incompressible Navier-Stokes equations", *Comput. Methods Appl. Mech. Engrg.* **105**, 285-298 (1993).
- [10] W.C. Moss, D.B. Clarke, and D.A. Young, "Calculated Pulse Widths and Spectra of a Single Sonoluminescencing Bubble", *Science* **276**, 1398 (1997).

- [11] R. Taleyarkhan, private communication (1998).
- [12] Y.B. Zel'dovich and Y.P. Raizer, "Physics of Shock Waves and High-Temperature Hydrodynamic Phenomena", Academic Press, New York, (1996).
  - [13] F.H. Ree, "Equation of State of Water", LLNL Report, UCRL-52190 (1976).
- [14] G.A. Gurtman, J.W. Kirsch, and C.R. Hastings, "Analytical Equation of State for Water Compressed to 300 Kbar", *Journal of Applied Physics*, **42**, 851 (1970).
- [15] M.H. Rice and J.M. Walsh, "Equation of State of Water to 250 Kilobars", *The Journal of Chemical Physics*, **26**, 824 (1957).
- [16] S. Bae, "A Theoretical Investigation of the Dynamics of Single Bubble Sonoluminescence", PhD Thesis Engineering Physics, Rensselaer Polytechnic Institute (1999).
- [17] B.P. Barber, C.C. Wu, R. Lofstedt, P.H. Roberts and S.J. Putterman, "Sensitivity of Sonoluminescence to Experimental Parameters", *Phys. Rev. Lett.*, 72, 1380 (1994).
- [18] G. Delgadino, "The Dynamics of Single Bubble Sonoluminescence", PhD ThesisEngineering Physics, Rensselaer Polytechnic Institute (1999).
- [19] W.C. Moss, D.B. Clarke, J.W. White and D.A. Young, "Hydrodynamic Simulation of Bubble Collapse and Picosecond Sonoluminescence", *Phys. Fluids*, 6, 2979 (1994).
- [20] Z. Johan, T.J.R. Hughes, and F. Shakib, "A globally convergent matrix-free algorithm for implicit time marching schemes arising in finite element analysis", *Computer Methods Applied Mechanics and Engineering* **87**, 281-304 (1991).



Figures 5 Spatial profiles of various parameters at three times  $(t_0,\,t_1,\,\text{and}\,\,t_2)$  before  $T_{max}$  occurs, and one time  $(t_3)$  after  $T_{max}$  occurs  $(T_{max}$  is the maximum temperature due to strong shock rarefaction at the center of the bubble). Adiabatic conditions assumed for an oscillating air bubble.

Figure 6 Example of location of interface with indicator function,  $\boldsymbol{F}$